Transport of passive tracers by monopoles on the β-plane

A. Bracco

Istituto di Cosmogeofisica - Corso Fiume 4, 10133 Torino, Italy

Summary. — We investigate the transport properties of monopolar coherent vortices in Rossby wave barotropic turbulence, exploring the role of a finite Rossby deformation radius. Isolated monopoles can trap tracers releasing them at a different latitude and sufficiently strong free-surface effects can inhibit Rossby waves emission by the vortices. In environments with a finite Rossby deformation radius, as in the ocean, coherent structures can survive for very long time even in the presence of strong differential rotation, without releasing what is trapped in their interior.

PACS 47.27.Eq – Turbulence simulation and modeling.
PACS 47.32 – Rotational flow and voriticy.
PACS 47.32.Cc – Vortex dynamics.

1. – Introduction

The dynamical of fluids on a rapidly rotating planet, such as Earth, is significantly influenced by the planetary rotation. When rotation is coupled with strong stable stratification, the vertical component of the velocity field is appreciably weaker than the two horizontal ones. As a consequence, the large-scale motion of oceanic and atmospheric flows tends to become approximately two-dimensional on a local horizontal plane.

Quasi-geostrophic flows at high Reynolds number, $Re = \dfrac{UL}{\nu}$, where U is the typical velocity scale of the flow, L is the domain scale and ν is the viscosity coefficient, are characterized by the spontaneous emergence of coherent vortices [1-4] with lifetimes longer that the characteristic timescale of the nonlinear turbulent interactions. The coherent vortices contain most of the energy and enstrophy of the system [5, 6] and they extend their influence to the whole field [7].

In particular, the presence of coherent vortices affects the dynamics of passively advected tracers. A vortex acts as a barrier to particle exhange between the inside and the outside of the vortex itself and it enhances the transport of material properties in its core (see, *e.g.*, Elhmaïdi *et al.* [8], Babiano *et al.* [9], Provenzale [10]).

In two-dimensional turbulence, passive particles initially seeded in a coherent vortex remain inside the vortex core the vortex core for long periods of time, and they are ejected mainly during vortex-vortex interactions, when vorticity filaments are

formed. Particles initially seeded outside vortex cores (*i.e.* in the background), tend not to enter the coherent structures. This impermeability induces strong inhomogeneities in the particle distribution even for long times, and, possibly, strong differences between Eulerian and Lagrangian statistics over times longer than the typical eddy turnover time.

Intense, isolated vortices are frequently observed in many regions of the Earth's ocean and play a significant role in the trasport of heat and salinity. A well-known type of ocean vortices are the rings observed in the region of the North Atlantic Ocean, south and east of the Gulf Stream [11], or in the Kuroshio current extention in the North Pacific [12]. They are characterized by a strong nonlinearity (*i.e.* the ratio of the Rossby number associated with nonlinear advection and linear wave propagation, $U/(\beta l^2)$, is much greater than one), and by a long lifetime (rings have been observed for more than two years before they are reabsorbed in the main current).

In this paper, we address the problem of transport by monopolar coherent vortices in quasi-geostrophic turbulence. We shall investigate how differential rotation and free-surface effects affect the dynamics of monopoles. The paper is organized as follows. In sect. **2** the equations of quasi-geostrophic turbulence are introduced. In sect. **3** we discuss the dynamics of monopoles on the β-plane, and in sect. **4** we present the analysis of numerical simulations performed for different values of β and R the Rossby deformation radius. A discussion of the findings concludes the work.

2. – Dynamics of barotropic turbulence

The quasi-geostrophic approximation (see for example [13,14] for a complete derivation) describes the motion of a rotation-dominated, strongly stratified flow on a local horizontal plane.

In the following, we consider the equation of motion for a divergenceless, homogeneous flow. Vertical derivatives and the vertical velocity component vanish.

On a spherical planet, the Cartesian reference frame (x, y) is defined on the plane of motion such that the variable $x = (\phi - \phi_0) R_E \cos \theta_0$ refers to zonal (East-West) variations and $y = (\theta - \theta_0) R_E$ varies with latitude in the meridional (North-South) direction. Here ϕ_0 and θ_0 are the reference longitude and latitude at the center of the domain of interest, and R_E is the radius of the Earth.

The equation of motion for freely-decaying barotropic turbulence in the quasi-geostropic approximation is written in dimensionless variables as

$$(1) \qquad \frac{Dq}{Dt} = \frac{\partial q}{\partial t} + J[\psi, q] = D ,$$

where $\dfrac{D}{Dt}$ is the total advective derivative, $J[\psi, q] = \partial_x \psi \partial_y q - \partial_y \psi \partial_x q$ is the two-dimensional Jacobian operator, ψ is the streamfunction and

$$q = \omega + f_0 + \beta y - \psi/R^2$$

is potential vorticity. D is a generic dissipative term. The dissipative term D represents either molecular or eddy viscosity. In the latter case D considered as a parametrization of unresolved small-scale turbulent dynamics.

In this approximation, relative vorticity is defined as

$$\omega = \nabla^2 \psi$$

and consistently, the velocity field $\mathbf{u} = (u, v)$ is given by $u = -\partial_y \psi$ and $v = \partial_x \psi$.

The Coriolis parameter is defined as $f = 2\Omega \sin \theta$, where Ω is the rotation frequency of the Earth. In the quasi-geostrophic approximation, only the vertical projection of the Earth's rotation vector is taken into account. Thus this approximation looses validity near the Equator. As a simplication, f is often assumed to be a constant, *i.e.* $f = f_0 = 2\Omega \sin \theta_0$. An improved representation of the latitudinal variation of f can be obtained by expanding the Coriolis parameter in a Taylor series around the reference latitude θ_0. Differential rotation enters as a linear correction through the parameter $\beta = 2\Omega \cos \theta_0 / R_E$ and the Coriolis term becomes $f = f_0 + \beta y$. This approximation is referred to as β-plane. Near the Poles the β-effect is absent and quadratic corrections become important.

$R = R_0/L$ is the nondimensional Rossby deformation radius, where L is the size of the domain considered and $R_0 = \sqrt{gH}/f_0$. g and H are, respectively, the gravitational acceleration directed along the z-axis and the average depth of the fluid layer. The last term in the definition of potential vorticity is usually referred to as the free-surface contribution.

In the absence of dissipation ($D = 0$), equation (1) has an infinite number of conserved quantities, namely all vorticity moments, since the vorticity of each fluid element is an inviscid constant of motion. Among those quantities, there are two quadratic invariants, the mean energy E and the mean enstrophy Z, given by

$$(2) \qquad E = \frac{1}{2L^2} \int (\nabla \psi)^2 \, \mathrm{d}x \, \mathrm{d}y \,,$$

$$(3) \qquad Z = \frac{1}{2L^2} \int (\nabla^2 \psi - \psi/R^2)^2 \, \mathrm{d}x \, \mathrm{d}y \,,$$

where L is the size of the (square) domain.

The simultaneous conservation of these two quantities induces a direct cascade of enstrophy towards small scales and an inverse cascade of energy from small to large scales [15-17].

The spontaneous emergence of coherent vortices in an initially structureless vorticity field is the most striking feature of QG turbulence. The first clear evidence of this phenomenon was obtained by McWilliams [1], although strong indication were provided in earlier studies [18, 19]. The development of long-lived coherent structures is associated with the inverse energy cascade, as revealed by numerical simulations and laboratory experiments [1, 20], even if the energy transfer energy is not enough to explain why long-lived vortices are generated. Once vortices have formed, they dominate the dynamics. Their presence tends to suppress the turbulent cascades [5], and they carry most of the energy and the enstrophy of the flow.

The introduction of a latitudinal variation of the Coriolis parameter, associated with $\beta \neq 0$, leads to a turbulent flow with fewer and less intense vortices. In particular, differential rotation is responsible for the existence of an upper scale, $L_\beta = (U/\beta)^{1/2}$,

where U is the typical velocity scale of the flow, called the Rhines scale, above which the inverse energy cascade is inhibited[21]. Below the Rhines scale, vortices live shorter and emit Rossby waves, undergoing zonal and meridional motion.

3. – Monopoles on the β-plane

Any isolated circular, symmetric monopolar vortex is stationary in the absence of forcing, dissipation and variation of the Coriolis parameter, implying that the monopole does not transport fluid by itself. On the other hand, the variation of the Coriolis frequency with latitude induces a dipolar vorticity anomaly superimposed on the vortex, and the whole structure translates just as in the case of a dipolar vortex. The coupling of two closed counter-rotating vortices provides a non-zero net linear momentum, causing the dipole to propagate in a direction which depends on the relative intensity and location of the two coherent structures.

However, the evolution of a monopole on the β-plane is more complicated than dipole dynamics, because a circularly-symmetric monopole on the β-plane is not a stationary structure in any reference frame. The initial vorticity distribution is distorted by stretching and compression of its fluid columns as they circle around the center of the vortex. Dynamically, the effect is the same as in case of a monopole placed over a bottom slope in a rotating fluid.

Another difficulty arises from the production of a wake which interacts with the monopole, due to the radiation of Rossby waves[22-24].

In the following, we consider the evolution of an initial Gaussian profile of relative vorticity

$$(4) \qquad\qquad \omega_{\text{init}} = \omega_m \exp[-r^2],$$

exploring different differential rotation rates (*i.e.* different values of β) and the influence of a finite Rossby deformation radius. The initial vorticity field has kinetic energy $E(t=0)=0.5$ and averaged enstrophy $Z(t=0)=5.6$, which implies a typical eddy-turnover time $T_e = Z^{-1/2} \approx 0.4$.

Equation (1) with $F=0$ is numerically integrated on a doubly periodic domain with size $[2\pi, 2\pi]$ and resolution 512^2 grid points using a pseudo-spectral code with a standard 2/3 dealiasing (see Canuto *et al.*[25] for detail on the numerics). The time integration is performed by a third-order Adams-Bashforth scheme. The dissipation term is provided by a biharmonic operator $D = -\nu_2 \nabla^4 \nabla^2 \psi$ (in the following $\nu_2 = 5\cdot10^{-8}$).

To study in detail the transport properties of monopolar vortices on the β-plane, passive Lagrangian particles having vanishing inertia with respect to the advecting fluid are seeded inside the vortex core.

Particle advection is performed by numerically solving the equations

$$(5) \qquad\qquad \frac{\mathrm{d}x}{\mathrm{d}t} = -\frac{\partial\psi}{\partial y}, \qquad \frac{\mathrm{d}y}{\mathrm{d}t} = \frac{\partial\psi}{\partial x},$$

where $\mathbf{x}(t) = [x(t), y(t)]$ is the particle position at time t and $\mathbf{v} = \left(-\frac{\partial\psi}{\partial y}, \frac{\partial\psi}{\partial x}\right)$ is the Eulerian velocity at point (x, y) and at time t.

The particle motion is integrated in time using a third-order Adams-Bashford

scheme and the Eulerian velocities are interpolated at the particle position by a third-order spline.

The study of absolute and relative dispersion provides information on the particle advection. Absolute (or single-particle) dispersion mesasures the mean square displacement of individual particles at time t and is defined as

(6) $$A^2(t; t_0) = \langle |\mathbf{x}_i(t) - \mathbf{x}_i(t_0)|^2 \rangle,$$

where $\langle * \rangle$ is an ensemble average over many particles, $\mathbf{x}_i(t)$ is the position of the i-th particle at time t, and t_0 is the time at which particles have been released.

Relative dispersion measures the mean square displacement at time t between a pair of particles released close to each other at time t_0. It is defined as

(7) $$D^2(t; t_0) = \frac{1}{2} \langle |\mathbf{x}_i(t) - \mathbf{x}_{i+1}(t)|^2 \rangle,$$

where $\langle * \rangle$ now indicates average over pairs of particles.

Flows on the β-plane are anisotropic and dispersion along x and y are different. Thus, the two components of the square of the displacement must be considered separately.

4. – Results

4˙1. *Weak differential effects.* $\beta = 4$. – Nondimensional parameter values are set as

$$\beta = 4 ; \qquad \frac{1}{R^2} = 0 .$$

The characteristic Rossby wave period, $T_R = 2\pi/\beta$, is approximately 1.6. The vortex is strongly nonlinear with a slow rate of frictional decay.

The numerical solution is illustrated in fig. 1. Over the integration up to time $t = 50.5$, the vortex has propagated to the northwest. Fluid from the outer rings of the vortex is peeled off while it moves up, and left behind in form of a weak Rossby wave wake, but the core of the coherent structure keeps its individuality. An annulus of negative potential vorticity surrounds the propagating vortex at time 3 (fig. 1a). Inside the cyclon initially all fluid particles move in counter-clockwise direction. The fluid elements in the annulus are advected in the same sense, in agreement with the experimental results obtained by Carnevale & Kloosterziel [23]. In the annulus, the vorticity of the fluid elements which are advected to the north has to become more negative to conserve potential vorticity. The part of the annulus on the northeast side strengthens and a center of negative vorticity forms. The fluid between the positive core and the new negative concentration is advected between the two opposite extrema. This results in the creation of a dipole tail, as is seen both in panel (a) and (b). This process of generating new vortical regions of alternating sign continues (in panel (b) already three stage can be indentified) and creates Rossby wave vorticity wakes that are slowly dissipated (panel (c)). Note that during the whole evolution, the annulus remains strongest on the northeast side of the core, inducing a continuous northwestward motion.
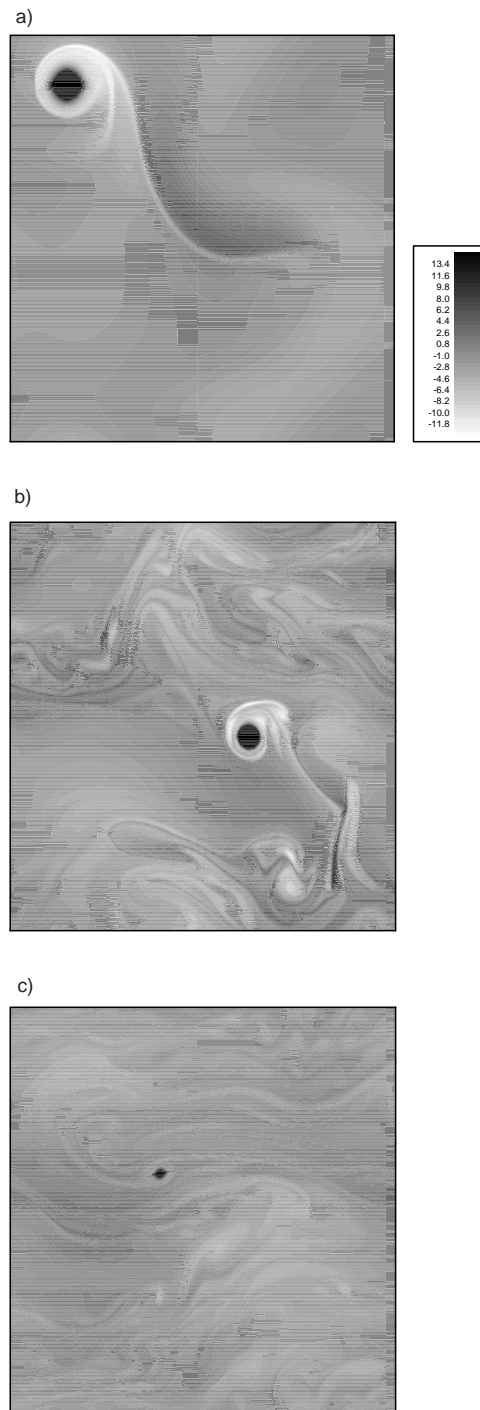
a)

b)

c)

Fig. 1. – Temporal evolution of the potential vorticity field for a northward propagating monopole on the β-plane when $\beta = 4$ and $R = \infty$. Panel (a) shows the vorticity field at time $t = 3$, panel (b) at time $t = 15$, panel (c) at time $t = 50$.
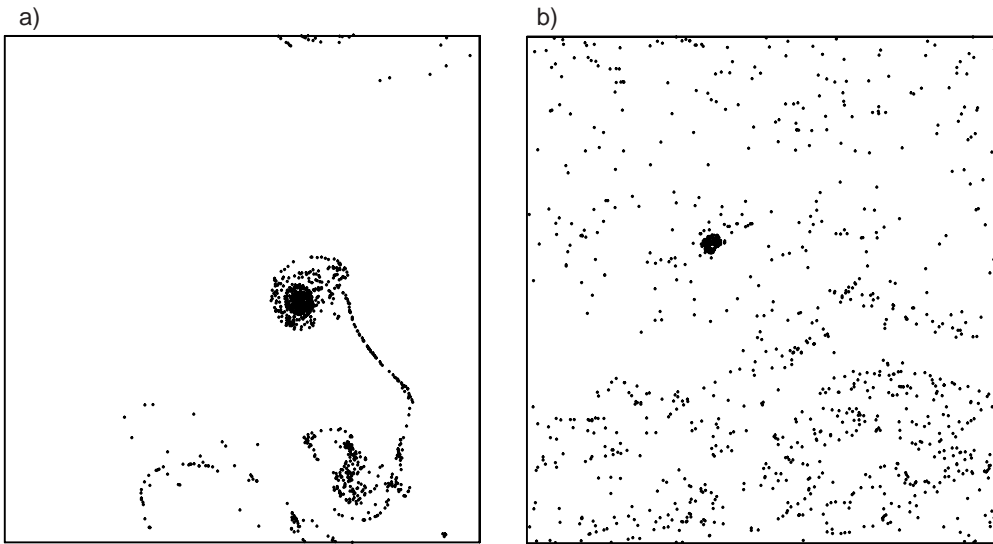
Fig. 2. – Temporal evolution of 1000 passive Lagrangian tracers initially released inside the coherent monopole. Panel (a) shows the particle distribution at time $t = 15$, panel (b) at time $t = 50$. Here $\beta = 4$ and $R = \infty$.

On the whole, however, this isolated vortex remains an individual structure for a long time (a nondimensional interval of 50.5 corresponds to ≈ 125 eddy rotation periods).

Particles released in concentric circles inside the vortex at time $t = 0$ remain all concentrated in the coherent structure until time $t \approx 4$. Panel (a) of fig. 2 shows the particle distributions at time $t = 15$. Lagrangian tracers draw the dipole structure of the tail and the negative vorticity lobes surrounding the vortex core. At time $t = 50$ one can still identify a small clump of particles in correspondence of the vortex core, while most of the tracers are spread out in the background field.

The relative dispersion of particle pairs initially placed in five different concentric circles is shown in fig. 3. Panel (a) refers to zonal and panel (b) to meridional dispersion. Particle pairs separate very little until they remain inside the vortex. As time goes on, however, the different concentric circles are sequentially ejected and relative dispersion grows fast after ejection. A marked asymmetry between zonal and meridional transport is observed once Lagrangian tracers are ejected by the monopolar vortex.

Rossby waves tend to move passive constituents mainly along the zonal direction, and meridional dispersion for pairs initially placed in the outer circles saturates after time $t \approx 20$. By contrast, the coherent monopole has a significant meridional component in its motion. Passive particles initially seeded inside the vortex are also displaced meridionally and are released at different stages of the vortex disruption at different latitudes with respect to their original location. The trapping of passive tracers inside coherent monopoles on the β-plane provides a possible mechanism for meridional mixing.
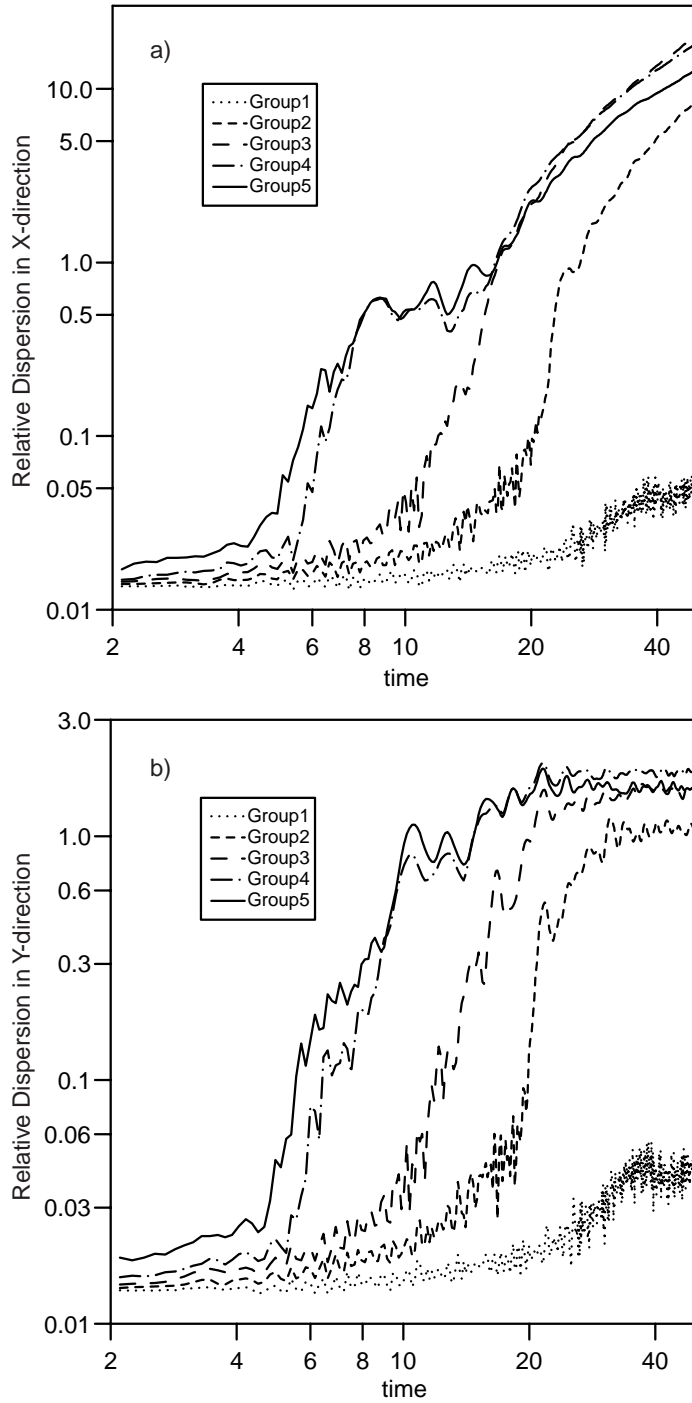
Fig. 3. – Relative dispersion along x (panel (a)) and y (panel (b)) for particle pairs initially released in concentric circles from the core (Group1) to the edge (Group 5) of the coherent vortex. Here $\beta = 4$ and $R = \infty$.
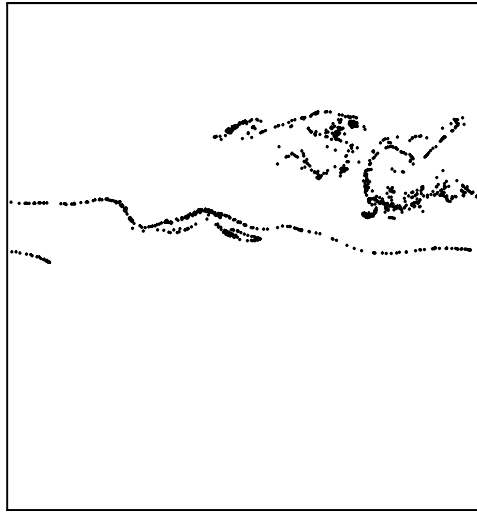
Fig. 4. – Lagrangian distribution at time $t = 7.5$ of a cloud of 1000 tracers initially placed inside a coherent monopole. Here $\beta = 32$ and $R = \infty$.

4'2. *Strong differential effects.* $\beta = 32$. – For larger values of β, such as

$$\beta = 32 \; ; \qquad \frac{1}{R^2} = 0$$

and for the same initial relative vorticity configuration, linear Rossby waves dominate the dynamics of the flow.

The vortex emits waves and strong vorticity filaments, and lives for a few rotation times. The particle distribution (fig. 4) shows that transport in the meridional direction is inhibited and tracers move mainly along the zonal direction.

We next explore how a finite Rossby deformation radius affect the dynamics.

Free-surface effects slow down the inverse energy cascade at scales larger than R. As a result, the dynamics becomes spatially more localized [26, 27]. Vortices are "incapsulated" in domains with typical size R. Inside each domain the dynamics is basically as for quasi-geostrophic turbulence, but different domains interact weakly with each other.

On the β-plane, Rossby wave formation is inhibited and vortices can live longer whenever the Rossby deformation radius is comparable with or smaller than the Rhines scale.

For

$$\beta = 32 \; ; \qquad \frac{1}{R^2} = 10$$

(*i.e.* for a Rossby deformation radius $R \approx 0.3$, one third of the domain size), the evolution of a vortex monopole does not show significant differences compared to the previous case, where free-surface effects were not taken into account. The coherent
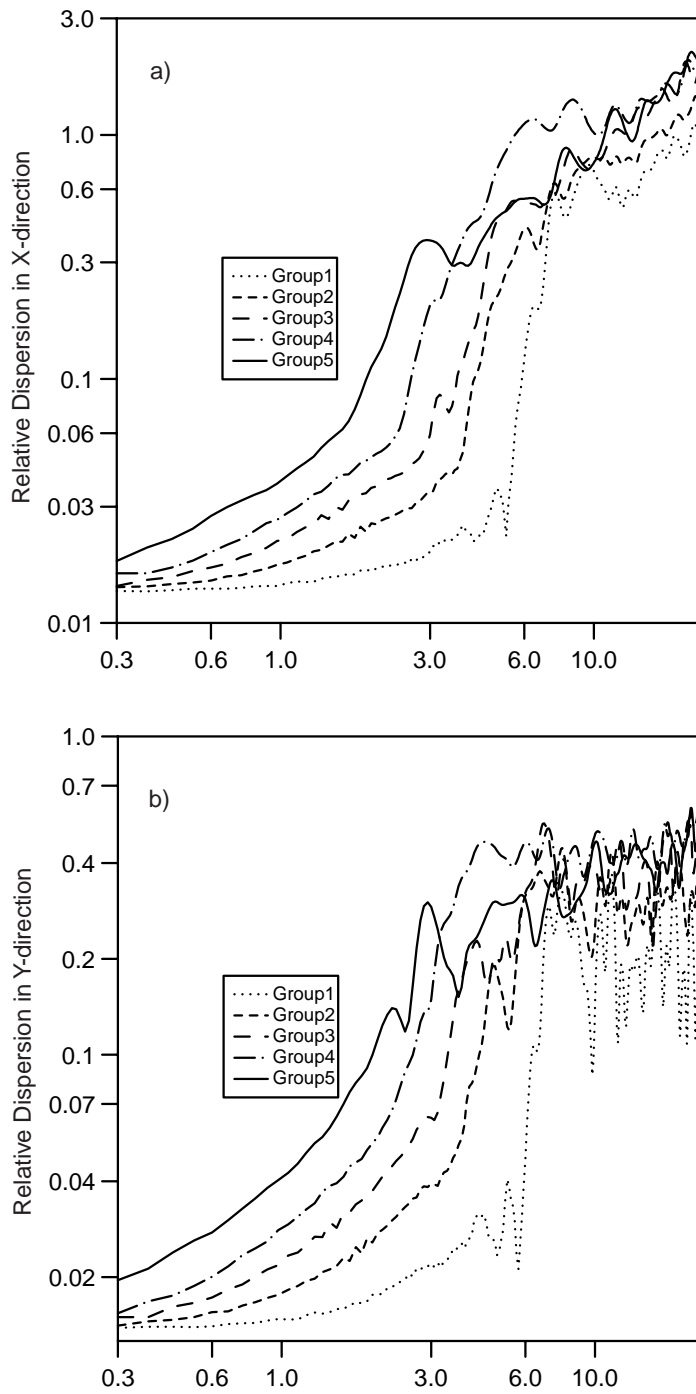
Fig. 5. – Relative dispersion along x (panel (a)) and y (panel (b)) for particle pairs initially released in concentric circles from the core (Group1) to the edge (Group 5) of the coherent vortex. Here $\beta = 32$ and $R \approx 0.3$.
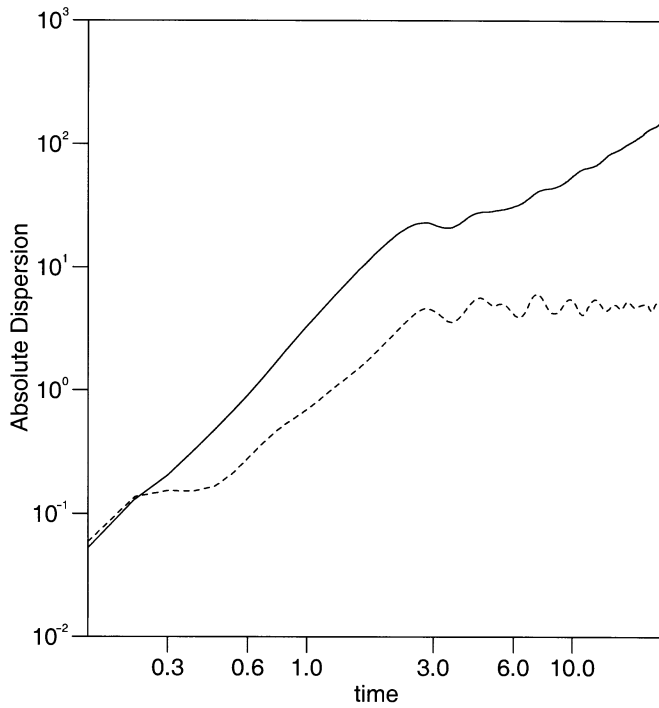
Fig. 6. – Absolute dispersion along x (solid line) and y (dotted line) for particles released in concentric circles inside the coherent monopole at time $t = 0$. Here $\beta = 32$ and $R \approx 0.3$.

vortex undergoes zonal and meridional motion, emitting Rossby waves, and it looses its individuality after few turnovers.

The relative dispersion of Lagrangian tracers initially seeded inside the monopole in concentric circles reveals again a strong asymmetry between zonal and meridional displacements (fig. 5). Dispersion in the zonal direction continuously grows in time, while particles tend to remain close to the latitude where they were released during the vortex filamentation processes. The discrepancy is more evident from the analysis of absolute dispersion (fig. 6). No significant differences between zonal and meridional dispersion are evident until tracers are ejected from the vortex core. After time $t \approx 4$, however, A_y^2 along the y-axis oscillates around a fixed value. The oscillatory behavior is due to Rossby wave progation. By contrast, single-particle dispersion in the zonal direction takes approximately the standard Brownian form $A_x^2(t) = 2Kt$ at large times, where K is the dispersion coefficient [28].

When further decreasing the Rossby deformation radius, $i.e.$

$$\beta = 32 \; ; \qquad \frac{1}{R^2} = 25 \; ,$$

(R = one-fifth of the domain size), the evolution of the monopolar vortex displays a substantial change. For these parameter values, Rossby waves wake turbulence does not dominate the field. The vortex monopole (fig. 7a) maintains its identity during the whole integration period (the numerical integration is performed until time $t = 50$).
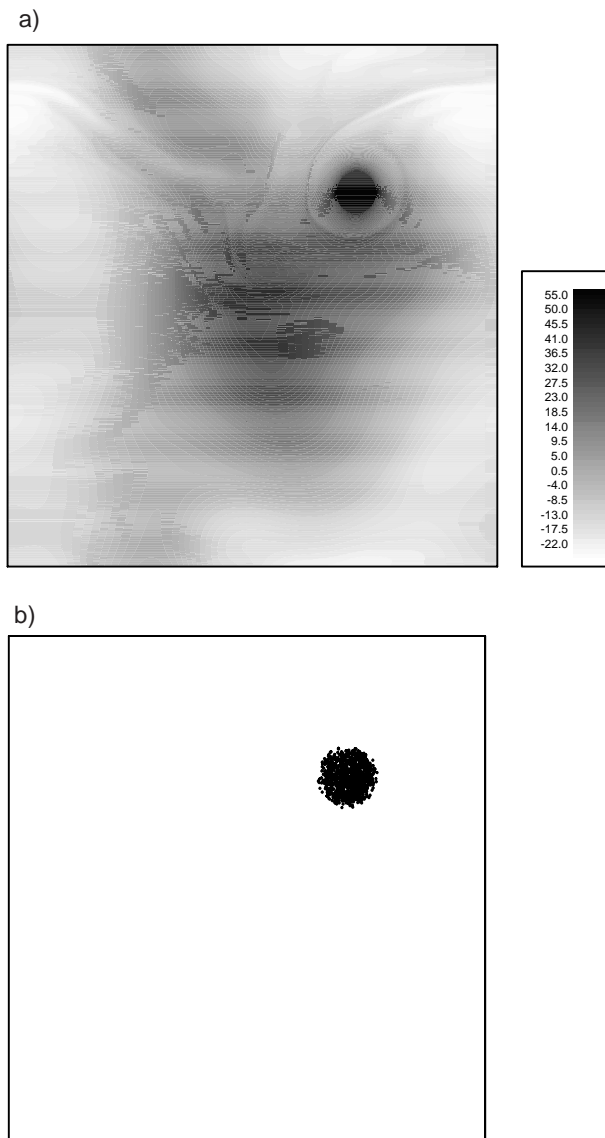
a)

b)

Fig. 7. – Potential vorticity field (panel a) and Lagrangian passive tracers (panel b) at time $t = 22$. Here $\beta = 32$ and $R = 0.2$.

Particles initially released inside the coherent structure remain clumped together until the end of simulation, displaying almost null relative dispersion both in the zonal and meridional directions.

Thus, the presence of a free-surface has a stabilizing effect on the dynamics of vortices on the β-plane. When the Rossby deformation radius is small enough, even relatively weak vortices (*i.e.* vortices such that the advection term they generate is weak compared to the β (linear) term in eq. (1)) may survive for a long period. These vortices can travel long distances and induce significant effects on transport because of

the meridional component of their motion. Particles as well as material concentrations can be released at a different latitude with respect to their original location. For the time they preserve their identity, mixing and biological or chemical reactions between the inside of the coherent structure and the outer regions are inhibited.

5. – Conclusion

Vortices can trap fluid particles and transport them during their motion for long times. Even in Rossby wave turbulence isolated monopoles, which display meridional motion, can trap tracers and/or passive materials, releasing them at a different latitude. Free-surface effects, if sufficiently strong, inhibit Rossby waves emission by the vortex, preserving the coherent structure from disappearing on short times.

* * *

REFERENCES

[1] McWilliams J. C., *J. Fluid Mech.*, **146** (1984) 21.
[2] McWilliams J. C., *J. Fluid Mech.*, **219** (1990a) 361.
[3] Babiano A., Basdevant C., Legras B. and Sadourny R., *J. Fluid Mech.*, **183** (1987) 379.
[4] Marteau D., Cardoso O. and Tabeling P., *Phys. Rev. E*, **51** (1995) 5124.
[5] McWilliams J. C., *Phys. Fluids*, **2** (1990b) 547.
[6] Bartello P. and Warn T., *J. Fluid Mech.*, **326** (1996) 357.
[7] Bracco A., Lacasce J., Pasquero C. and Provenzale A., *Phys. Fluids*, **12** (2000) 2478.
[8] Elhmaïdi D. A., Provenzale A. and Babiano A., *J. Fluid Mech.*, **257** (1993) 533.
[9] Babiano A., Boffetta G., Provenzale A. and Vulpiani A., *Phys. Fluids*, **6** (1994) 2465.
[10] Provenzale A., *Ann. Rev. Fluid Mech.*, **31**, (1999) 55.
[11] Parker C., *Deep Sea Res.*, **18** (1971) 981.
[12] Cheney R. E. and Richardson P. L., *POLYMODE News*, No. 31 (1977).
[13] Charney J. G., *J. Atmos. Sci.*, **28** (1971) 1087.
[14] Pedlosky J., *Geophysical Fluid Dynamics*, Springer-Verlag 710 pp. (1987).
[15] Kraichnan R. H., *Phys. Fluids*, **10** (1967) 1417.
[16] Batchelor G. K., *Phys. Fluids Suppl.*, **12** (1969a) II-233.
[17] Kraichnan R. H. and Montgomery D., *Reports Progr. Phys.*, **43** (1980) 547.
[18] Fornberg B., *J. Comput. Phys.*, **25** (1978) 1.
[19] Basdevant C., Legras B., Sadourny R. and Beland M., *J. Atmos. Sci.*, **38** (1981) 2305.
[20] Tabeling P., Burkhart S., Cardoso O. and Willaime H., *Phys. Rev. Lett.*, **67** (1991) 3772.
[21] Rhines P. B., *J. Fluid Mech.*, **69** (1975) 417.
[22] McWilliams J. C. and Flierl G. R., *J. Phys. Ocean.*, **9** (1979) 1155.
[23] Carnevale G. F. and Kloosterziel R. C., *Physica D*, **76** (1994) 147.
[24] Sutyrin G. G., Hesthaven J. S., Lynov J. P. and Rasmussen J. J., *J. Fluid Mech.*, **268** (1994) 103.
[25] Canuto C., Hussaini M. Y., Quarteroni A. and Zang T. A., *Spectral Methods in Fluid Dynamics* (Springer-Verlag, Berlin) 1987.
[26] Polvani L. M., Zabusky N. J. and Flierl G. R., *J. Fluid Mech.*, **225** (1989) 241.
[27] Larichev V. D. and McWilliams J. C., *Phys. Fluids*, **3** (1991) 938.
[28] Taylor G. I., *Proc. London Math. Soc.*, **20** (1921) 196.